JOURNAL OF COLLOID AND INTERFACE SCIENCE **180,** 504–518 (1996)
ARTICLE NO. 0331

# Ultrafiltration of Colloidal Dispersions—A Theoretical Model of the Concentration Polarization Phenomena

ANN-SOFI JÖNSSON[1] AND BENGT JÖNSSON[2]

*Department of Chemical Engineering I, Lund University, P.O. Box 124, S-221 00 Lund, Sweden*

Received July 10, 1995; accepted December 27, 1995

**A general thermodynamic model of the concentration polarization phenomena of colloidal particles at a membrane surface is presented. The model is based on the balance between a thermodynamic force, due to the osmotic pressure gradient, and a frictional force, due to the fluid flow around each particle. A cell model description is used to model the concentration dependence of the thermodynamic force as well as the flow properties in the concentrated colloidal solution. Equilibrium thermodynamics of the colloidal system can be used in the cell calculations since local equilibrium is assumed in the neighborhood of each colloidal particle (i.e., in each cell). This means that the concentration dependence of the osmotic pressure can be obtained, either from an experimental determination or from a theoretical model of the bulk properties of the colloidal system. To exemplify the usefulness of the model when establishing the influence of different operating parameters, such as the transmembrane pressure, the fluid shear, or different solution properties, such as concentration, particle size, pH, and ionic strength, a model system of charged spherical colloidal particles is used. The interaction between the particles is in the presented examples assumed to be a combination of electrostatic interactions, calculated from the Poisson–Boltzmann equation, dispersion forces, calculated as additive $1/r^6$ interactions, and a hard sphere interaction calculated from the Carnahan–Starling equation.** 

*Key Words:* **colloids; flow model; osmotic pressure; concentration polarization; ultrafiltration.**

## INTRODUCTION

Membrane separation processes are used in a wide variety of industrial applications, for separation of ions, macromolecules, and colloids (1–4). During the past years, the commercial value of membrane processes has grown very fast, mainly due to increasingly stringent environmental demands and the striving for the zero discharge manufacturing plant. The most important advantages of membrane processes are their unique separation capabilities and the low energy consumption. However, membrane separation processes are very complex processes, influenced by several operating parameters, and it is thus difficult to predict the membrane performance in different applications, although more elaborate theoretical models are constantly presented (5–12). When predicting the capacity of a membrane plant it is essential that the flow resistance caused by retained solute molecules accumulated at the membrane surface can be calculated accurately. However, when treating colloidal suspensions, the traditionally used models, derived for separation of low-molecular solutes, cannot be used. In this case the thermodynamic properties characterizing the specific colloidal system must be considered.

In this paper a cell model is used to calculate the concentration polarization at the membrane surface. Calculations based on cell models have been very successful in other systems, both when describing the thermodynamic equilibrium properties, such as the osmotic pressure and other chemical potentials in colloidal systems (13–14), and when describing diffusion or fluid flow through concentrated suspensions (15–16). In this paper the cell model is used to calculate the concentration profile of colloidal particles outside the membrane surface by assuming that there is always a local equilibrium in the neighborhood of each colloidal particle (i.e., in each cell). Using the cell model, the influence of operating parameters, such as the fluid flow, the concentration of colloidal aggregates, and the net charge of the aggregates, is calculated. Before presenting the new concentration polarization model, a short summary of how polarization phenomena are treated traditionally is given below.

The concentration gradient in the boundary layer adjacent to the membrane is usually described by the cake filtration, or the osmotic pressure, model. In the cake filtration model a cake with constant solute concentration, and in the osmotic pressure model an exponential concentration of solute molecules, is assumed at the membrane surface. The fundamental aspects of these models have been discussed in a vast number of articles, for example, (17–24).

In the cake filtration model it is assumed that a layer of concentrated solute, a cake, is formed on the membrane. The flux, $J$, is then supposed to be reduced due to the additional

[1] To whom correspondence should be addressed.

[2] Current address: Department of Physical Chemistry 1, Lund University, P.O. Box 124, S-221 00 Lund, Sweden.



0021-9797/96 $18.00

flow resistance offered by the cake. The flux is expressed as

$$J = \frac{\Delta P}{\eta(R_m + R_c)}, \quad [1]$$

where $\Delta P$ is the pressure difference across the membrane, $\eta$ is the viscosity, and $R_m$ and $R_c$ are the hydraulic resistances of the membrane and the cake, respectively.

In Eq. [1] it is assumed that the cake is incompressible and that the osmotic pressure at the surface of the cake can be neglected. The osmotic pressure may, however, be substantial, not only for low-molecular solutes, but also for macromolecules and colloidal dispersions (20, 24–25).

In the osmotic pressure model the osmotic pressure is included in Eq. [1] and the flux is then described as

$$J = \frac{(\Delta P - \Delta\Pi)}{\eta R_m}, \quad [2]$$

where $\Delta\Pi$ is the transmembrane osmotic pressure difference. The van't Hoff law is usually used to correlate the transmembrane osmotic pressure and concentration difference. However, the van't Hoff law only applies for ideal solutions, and empirical relations must therefore often be used.

A second equation that relates the flux, $J$, and the solute concentration at the membrane, $C_m$, can be obtained from the film theory (26). In the film theory, the fluid flow in the stagnant layer with thickness $\delta$ adjacent to the solid surface is assumed to be laminar, whereas the fluid flow outside of this layer is turbulent with complete mixing of the solute. The thickness of the stagnant layer depends on the shear forces and the rheological properties of the solution in a complicated manner and is usually integrated in the mass transfer coefficient which is obtained from experiments. At steady state the convective solute transport in the stagnant layer is equal to the permeate flow and the diffusive back transport of solute into the bulk solution.

$$J(C - C_p) = -D\frac{dC}{dx}, \quad [3]$$

where $C$ is the solute concentration, $C_p$ is the concentration in the permeate, $D$ is the diffusion coefficient, and $x$ is the distance from the membrane surface. Usually the diffusion coefficient is assumed to be independent of concentration and when Eq. [3] is integrated the following well-known correlation is obtained:

$$J = \frac{D}{\delta}\ln\left(\frac{C_m - C_p}{C_b - C_p}\right) = h_D\ln\left(\frac{C_m - C_p}{C_b - C_p}\right), \quad [4]$$

where $\delta$ is the thickness of the boundary layer, $h_D = D/\delta$ is the mass transfer coefficient, and $C_m$ and $C_b$ are the concentrations at the membrane surface on the feed side and in the bulk solution, respectively. The solute concentration at the membrane can be calculated from a combination of Eqs. [2] and [4] if the correlation between osmotic pressure and concentration is known.

A serious shortcoming of Eq. [3] is that the diffusive flow is written as $(-D\cdot dC/dx)$. This representation of the diffusive flow can be used only for solutions with noninteracting solutes (i.e., ideal solutions). In colloidal dispersions, with long-range interactions between the colloidal particles in the dispersion, the diffusive flow is proportional to $(-D\cdot C/kT\cdot d\mu/dx)$, where $k$ is the Boltzmann constant, $T$, the absolute temperature, and $d\mu/dx$, the derivative of the chemical potential of the particles. The fluid flow equations obtained from the cake filtration model and the osmotic pressure model do not include the concentration dependence of the diffusion coefficient, nor the nonideal concentration dependence of $\mu$ that is typical of a colloidal solution.

The cake filtration and the osmotic pressure models represent two extreme cases of how the concentration profile in the boundary layer adjacent to the membrane surface is built up during a membrane process. The osmotic pressure model applies fairly well when treating solutions containing small, noninteracting solutes, whereas when treating solutions containing macromolecules, or colloidal particles, the cake filtration model gives a better description of the concentration profile. However, for solutions containing solutes of intermediate size, as for example colloidal particles smaller than 0.1 $\mu$m, neither of these models describe the concentration profile accurately. These particles are too small to be described by the cake filtration model and the interactions between the particles, even at great distances, make the osmotic pressure model inappropriate.

Different models which describe membrane treatment of colloidal solutions have been proposed. Dejmek (27) was the first to discuss the force balance in a concentration polarization layer. Wijmans *et al.* (22) also used the force balance concept when they showed that the resistance of the boundary layer could be calculated from the solvent permeability of the colloidal solute. However, an exponential concentration profile is assumed in this work, an approximation originating from the assumption that the mass transfer due to diffusion only depends on the concentration gradient and not on the gradient of the chemical potential. Recently, Petsev *et al.* (7) presented a theoretical model of the ultrafiltration of concentrated dispersions of charged colloidal particles. In their model, the particles in the boundary layer are placed in a lattice and the force balance on each particle in the lattice is calculated. The equations describing the force between the particles are obtained from pair DLVO interparticle interactions and cell model hydrodynamics. A similar model is presented by Welsch *et al.* (11).

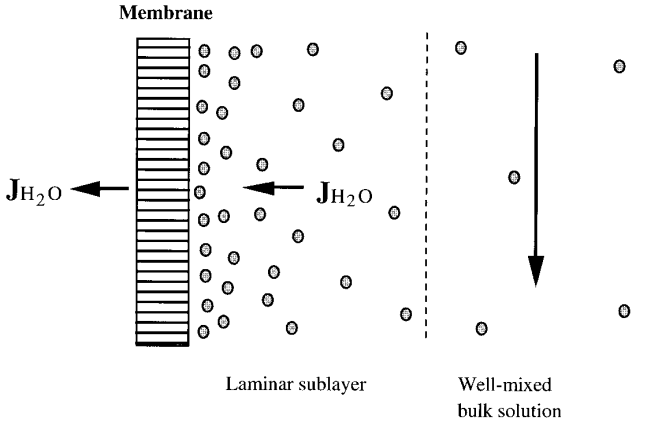


**FIG. 1.** Concentration polarization at the surface of an ultrafiltration membrane.

A novel dynamic model of ''dead-end'' ultrafiltration is presented by Bowen and Jenner (12). In this model the pressure within a filter cake is analyzed in terms of the local compressive drag and hydraulic forces on the particles in a layer. Models for particle–particle interactions are in the Bowen and Jenner model used to determine the compressibility properties of the cake.

The objective of the present study was to derive a fluid flow model which describes the concentration gradient, established during ultrafiltration, from experimentally easily obtainable system characteristic parameters, such as the concentration dependence of the osmotic pressure and diffusion/sedimentation coefficients. The model presented is based on a basic thermodynamic description of a colloidal system and can be used to describe concentration gradients during ultrafiltration of any type of colloidal dispersion, as long as the concentration dependence of the osmotic pressure and the diffusion/sedimentation coefficients are known. A similar model for hard sphere systems is presented in (28). Experiments have been performed on silica sols under different experimental conditions (29) and it is the properties of these solutions that have been used to illustrate the model in this work.

A theoretical discussion of the influence of different particle–particle interactions, such as the attractive van der Waals forces and the repulsive electrostatic forces, on the coagulation stability of colloidal dispersions during membrane filtration is also included.

## THE THEORETICAL MODEL

It is assumed that the diffusion and flow properties on the feed side of the membrane may be described by a film model, i.e., there is a thin laminar boundary layer adjacent to the membrane, and outside this sublayer the solution is well mixed with a constant solute concentration, as shown in Fig. 1. Material is transported by convection toward the membrane and away from the membrane by diffusion. This is probably an acceptable description of the system when treating colloidal dispersions with particles smaller than 0.1 $\mu$m. For solutions with larger particles, additional effects such as shear-induced diffusion and inertial lift start to be important (6, 30–33). However, these phenomena are beyond the scope of this paper.

A concentration profile is established in the laminar sublayer due to the transport of solute particles toward the membrane. At steady state the concentration profile has a shape such that the drag force exerted by the fluid flow around the particles in each layer outside the membrane is balanced by the thermodynamic force due to the concentration gradient over the layer, as shown in Fig. 2.

Concentrating on a single particle, the force balance gives

$$F_{ff} = F_{tf}, \qquad [5]$$

where $F_{ff}$ is the mean frictional force and $F_{tf}$ is the mean thermodynamic force on the particle.

Both the drag force and the thermodynamic force can usually be studied experimentally, independently of each other, and the influence of flow rate, particle concentration, electrolyte concentration, etc., can thus be determined for the two forces.

### *The Drag Force*

In dilute solutions, there is often a linear correlation between the drag force exerted by the fluid in motion around a particle and the fluid velocity relative to the particles, $v$.

$$F_{ff} = f_0 \cdot v \qquad [6]$$

The frictional coefficient, $f_0$, depends on the shape and size of the particle, as well as the viscous properties of the surrounding media. At high velocities the linear correlation between $F_{ff}$ and $v$ may collapse for different reasons, such as induced turbulence, deformation of the particle, and redis-

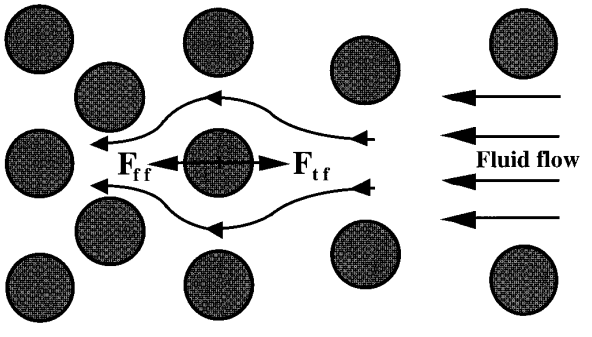


**FIG. 2.** Forces exerted on a particle. $F_{ff}$ denotes the drag force exerted by the fluid flow around the particle and $F_{tf}$ is the thermodynamic force due to the concentration gradient.

tribution of ions outside the particle. However, these effects are neglected in this model.

The frictional coefficient can be estimated either by measurement of the self diffusion coefficient or by measurement of the sedimentation constant. When the diffusion coefficient is measured, the Stokes–Einstein relation can be used to obtain a correlation between the diffusion coefficient of the particle, $D$, and the frictional coefficient, $f_0$ (34)

$$f_0 = \frac{kT}{D}, \qquad [7]$$

where $k$ is the Boltzmann constant and $T$ is the absolute temperature. The corresponding relation between the sedimentation constant, $S$, and the frictional coefficient, $f_0$, is (34)

$$f_0 = \frac{bM}{S \cdot N_A}, \qquad [8]$$

where $bM$ is the difference in mass between the particle and the displaced solvent and $N_A$ is Avogadro's number.

If there are no experimental self-diffusion or sedimentation data available, Stokes' relation can be used to estimate the frictional coefficient. For spherical particles in a dilute solution, the frictional coefficient becomes

$$f_0 = 6\pi\eta_0 r, \qquad [9]$$

where $r$ is the radius of the particle and $\eta_0$ is the viscosity of the solvent.

In concentrated dispersions, where the fluid flow around each particle is affected by other particles in the neighborhood, the frictional coefficient is strongly influenced by the concentration and also the correlation between the motion of the particles. It is also important to point out that the definition of the frictional coefficient, given in Eq. [6], is not suitable for use when dealing with concentrated solutions, since the velocity of the fluid relative to the particles is not constant, but varies as a function of the distance to the particles, and no well-defined velocity can be found. In concentrated dispersions at the surface of a membrane it is more convenient to define the frictional coefficient as the relation between the drag force and the average velocity of the surrounding fluid relative to the particle:

$$F_{ff} = f \cdot J \cdot (1 - \phi_p/\phi) \qquad [10]$$

where $\phi_p$ is the volume fraction of particles in the permeate and $\phi$ is the volume fraction of particles at the distance $x$ from the membrane surface.

Both the self-diffusion coefficient and the sedimentation constant can be used to estimate the frictional coefficient in dilute solutions, as mentioned above. However, in concentrated systems, the frictional coefficient may vary depending on whether it is estimated from self-diffusion or sedimentation data. The reason for this is that the velocity profile around a particle in a self-diffusion experiment and in a sedimentation experiment is different.

1. During *self-diffusion*, the long-term movement of the particles is physically uncorrelated, which means that the fluid flow around a particle can be described as the flow of a homogeneous fluid with an effective viscosity. If the rheological properties of the dispersion are known, the influence of concentration can, as a good approximation, be related to the viscosity of the dispersion, $\eta$, by

$$f/\eta \approx f_0/\eta_0, \qquad [11]$$

where $\eta_0$ is the viscosity in a dilute solution (35–36).

If no experimental data on the concentration dependence of the viscosity are available, a theoretical estimate can be used. For spherical particles, with no other interactions with the solvent than at the hard spherical surface, the Einstein equation can be used to describe the influence of concentration on viscosity, and, thus, on the frictional coefficient (37).

$$f = 6\pi\eta_0 r \frac{1 + 0.5\phi}{(1 - \phi)^2}. \qquad [12]$$

2. During *sedimentation*, the movement of the particles is physically correlated in the collective transport of particles through the medium. This is also the case when fluid flows through a lattice of stagnant particles, as in the boundary layer at the surface of a membrane. The frictional coefficient is, in this case, not related to the viscosity of the solution, as in Eqs. [11] and [12]. If no experimental sedimentation data are available, theoretical models must be used to estimate $f$. Happel (15) has shown, by the use of cell model calculations, that in this case the frictional coefficient can be expressed as

$$f = 6\pi\eta_0 r \cdot \frac{6 + 4\phi^{1.67}}{6 - 9\phi^{0.33} + 9\phi^{1.67} - 6\phi^2}. \qquad [13]$$

3. For stable, very concentrated dispersions, the frictional coefficient may be estimated through permeability measurements. By determining the pressure drop, $\Delta P$, per unit length, $\Delta L$, across a layer of colloidal particles as a function of the flux, $J$, through the layer, the frictional coefficient can be calculated from the relation

$$f = \frac{\Delta P}{\Delta L} \cdot \frac{V_{agg}}{\phi J}, \qquad [14]$$

where $V_{agg}$ is the volume of a particle and $\phi$ is the volume fraction of particles in the layer. A drawback with this method of determining the frictional coefficient is the need for very small fluid flows in order to minimize concentration gradients across the layer induced by the fluid flow through the layer.

In solutions containing charged particles, there are always counterions in the solution around each particle. In these cases, there may also be electroviscous forces that affect the frictional coefficient due to the fact that the fluid surrounding a charged particle is forced to flow through the double layer that surrounds the particle, which gives rise to a frictional force. It is very difficult to describe exactly the concentration dependence of this frictional term and we therefore refer the reader to (38) for a more detailed description of this phenomenon. The influence of the electroviscous effect on the frictional coefficient is, fortunately, not so dramatic. The influence of the electroviscous effect can usually be considered by assuming a slightly larger diameter, $r$, of the particles in the dispersion.

In order to obtain an easy-to-use expression for the concentration dependence of the frictional coefficient independent of whether experimental, or theoretical models are used, a series expansion in powers of the volume fraction, $\phi$, is used.

$$f(\phi) = \frac{6\pi\eta_0 r}{(1-\phi)^2} \cdot \sum_{i=0} f_i \phi^i, \qquad [15]$$

where the coefficients $f_i$ can be determined either experimentally or by a theoretical correlation of the type given in Eq. [13].

*The Thermodynamic Force*

The thermodynamic force on a particle is defined as the negative gradient of the chemical potential of the particles, $\mu_{agg}$ (34). Outside a membrane surface where the concentration of particles is constant along the surface, but varies perpendicular to the surface, the thermodynamic force can be expressed as

$$F_{tf} = -\left(\frac{d\mu_{agg}}{dx}\right)_T, \qquad [16]$$

where $x$ is the distance from the membrane surface.

In order to be able to use the above expression when deriving the concentration gradient at a membrane it is necessary to know how the chemical potential of the particles is affected by the concentration in the solution. This information is most easily obtained by determining the osmotic pressure in the bulk solution at different concentrations. The following equations can then be used to determine how $\mu_{agg}$ varies as a function of concentration.

(a) The relation between $d\mu_{agg}$ and $d\mu_w$, where $\mu_w$ is the chemical potential of the solvent, is obtained from the Gibbs–Duhem relation

$$N_{agg} d\mu_{agg} + N_w d\mu_w = 0, \qquad [17]$$

where $N_{agg}$ and $N_w$ are the number of particles and solvent molecules, respectively.

(b) Changes in the chemical potential of the solvent can also be expressed as a change in the osmotic pressure of the solution, $\Pi$. The following relation exists between these parameters:

$$d\mu_w = -V_w d\Pi, \qquad [18]$$

where $V_w$ is the volume of a solvent molecule. Combining Eqs. [16]–[18] gives

$$F_{tf} = -\frac{N_w V_w}{N_{agg}} \cdot \frac{d\Pi}{dx} = -V_{agg} \cdot \frac{(1-\phi)}{\phi} \cdot \frac{d\Pi}{dx}. \qquad [19]$$

(c) The osmotic pressure gradient outside a membrane, $d\Pi/dx$ in Eq. [19], is a result of the concentration gradient of colloidal particles in this region. To be able to estimate $d\Pi/dx$ the relation between osmotic pressure and concentration of colloidal particles must be known. This relation is often rather involved, depending on different particle–particle and particle–solvent interactions. However, the osmotic pressure of the solution can always be represented as a series expansion in powers of the particle concentration.

$$\Pi = \frac{kT}{V_{agg}} (\phi + \sum_{i=2}^{\infty} A_i \phi^i). \qquad [20]$$

In the van't Hoff law, often used to calculate the osmotic pressure in dilute solutions, all terms except the first one in the series expansion of Eq. [20] are neglected. The other contributions to the osmotic pressure may originate from, for example, steric, electrostatic, and/or van der Waals interactions between the particles. The constants $A_i$ in Eq. [20] can be either determined experimentally, for example, through osmometer measurements (25, 39–41), or determined from theoretical models (42). This problem is treated in more detail later, for the moment, we conclude that the osmotic pressure can be represented by a series expansion, as in Eq. [20]. Combining Eqs. [19] and [20] results in the following relation between the thermodynamic force and the concentration gradient:

$$F_{tf} = -kT\frac{(1-\phi)}{\phi}\left(1+\sum_{i=2}^{\infty}A_i i\phi^{i-1}\right)\frac{d\phi}{dx}. \quad [21]$$

*The Concentration Profile Equation*

Combining the expressions for the drag force, Eqs. [10] and [15], and the expression for the thermodynamic force, Eq. [21], with the force balance, Eq. [5], an equation for the concentration profile can be written as

$$J\cdot 6\pi\eta_0 r\cdot\sum_{i=0}^{\infty}f_i\phi^i = -kT\frac{(1-\phi)^3}{(\phi-\phi_p)}\left(1+\sum_{i=2}^{\infty}A_i i\phi^{i-1}\right)\frac{d\phi}{dx}. \quad [22]$$

This first-order differential equation is easily solved numerically when the values of the coefficients $f_i$ and $A_i$ are known. For an ideal, dilute solution where the frictional coefficient $f$ can be written as $f = kT/D_0$ and all the $A_i$ values in the concentration dependence of the osmotic pressure are zero, the above expression is reduced to the well-known relation

$$\frac{J}{D_0} = -\frac{(1-\phi)}{(\phi-\phi_p)}\frac{d\phi}{dx} \approx -\frac{1}{(C-C_p)}\frac{dC}{dx}. \quad [23]$$

This equation states that the concentration decreases exponentially at the membrane surface with a decay length $D_0/J$, as in Eq. [4]. However, Eq. [23] is valid only for ideal, dilute solutions; for a colloidal dispersion Eq. [22] must be used.

To be able to calculate the concentration profile at different flow velocities, electrolyte concentrations, etc., $\phi_p$, and the coefficients $f_i$ and $A_i$ in Eq. [22] must be determined. The best description of the concentration profile outside a membrane surface is, of course, obtained if experimental values of these variables are available. However, a theoretical model is useful to explain and illustrate the influence of different solution-specific parameters on the osmotic pressure. In the examples presented in this study, $\phi_p$ is assumed to be zero, Eq. [13] is used to calculate the coefficients $f_i$, and a model description of the concentration dependence of the osmotic pressure is used to determine the values of $A_i$ in Eq. [21].

*The Osmotic Pressure in a Colloidal Solution*

To be able to describe the influence of the particle concentration on the osmotic pressure in a dispersion, it is necessary to determine both the interaction between the particles and the distribution of particles in the solution. Today, there are no exact theoretical models relating these solution-specific parameters, but different approximate methods are available.

1. One commonly used method is to first determine the effective interaction between two single particles as a function of the distance between them and thereafter assume that the obtained relation is not affected by other particles in the solution (42–43). This is often a good approximation for dilute systems, independent of which types of interactions affect the particles. However, for concentrated systems, the interactions between two particles are often affected by other particles in the solution. This is especially pronounced when considering dispersions with ionic particles where the long-range electrostatic force is often the dominating particle–particle interaction.

2. A cell model is another way of thermodynamically describing a concentrated dispersion (44). In the cell model it is assumed that all particles in the solution are placed in a regular lattice so that the system can be divided into a number of uniform cells, each containing a particle with surrounding solvent. To simplify the calculations, the cell is usually approximated by a simple geometrical form such as a sphere, a spheroidal, or a cylinder (13). With the introduction of a simple geometrical cell shape, the calculation of the thermodynamic properties, such as the osmotic pressure and the chemical potential, is easily performed with standard numerical programs. The entropy due to the particle distribution is not included in the basic form of the cell model since the particles in the model are set out in a lattice. For large particles, this contribution can be neglected, but for small particles the entropy is of importance.

An estimation of this entropy contribution to the osmotic pressure of the colloidal system can, however, be obtained from the cell model calculations if the interactions between the particles are approximated by a concentration-dependent hard-sphere interaction (45). The reason for approximating the interaction with a hard-sphere interaction when estimating the particle entropy is that the so-called Carnahan–Starling equation (46) can be used to obtain a quite accurate relation for the concentration dependence of the osmotic pressure over a large concentration interval.

$$\Pi_{hs} = \frac{kT}{V_{agg}}\left(\frac{\phi_{hs}+\phi_{hs}^2+\phi_{hs}^3-\phi_{hs}^4}{(1-\phi_{hs})^3}\right), \quad [24]$$

where $\phi_{hs}$ is the volume fraction of the hard spheres. For systems with no long-range interactions between the particles, $\phi_{hs}$ can be replaced by the real volume fraction, $\phi$, and for these systems Eq. [24] can be used to determine the osmotic pressure due to the colloidal particles for concentrations less than $\phi \approx 0.5$. However, it must be pointed out that Eq. [24] also fails to predict the osmotic pressure in this concentration range if short-range interactions cause the particles to stick to each other in a porous structure. The properties of such systems are discussed in (47) but are, due to their complexity, omitted in this work. Instead we

have, as an approximation, assumed that Eq. [24] gives the entropic part of the osmotic pressure if the concentration of particles is less than the close-packing concentration (for a hexagonally close-packed dispersion $\phi_{cp} = \pi/\sqrt{18} \approx 0.74$). We have further assumed the particles to be incompressible which means that the osmotic pressure is assumed to be infinite for concentrations above $\phi_{cp}$.

$$\Pi_{hs} = \infty, \quad \text{when } \phi_{hs} > \phi_{cp}. \qquad [25]$$

If the concentration dependence in Eq. [24] is approximated by the linear term, the familiar van't Hoff equation is obtained. However, very few colloidal dispersions can be described as a collection of hard spheres with no long-range interactions between the particles. For most systems, there is at least some type of long-range interaction and the cell model may here be used to calculate the mean particle interaction as well as the interaction-dependent volume of the particles that is used to estimate the entropy of the particles. In this work, the effective volume of a particle is defined as the cell volume where the free energy of the system has increased by 1 $kT$ per particle compared with the original cell system.

The cell model is used in all examples presented in this paper since calculations based on this model have also proved to give a good description of thermodynamic quantities in concentrated systems, and the calculations are today easy to perform with standard programs.

Different interactions dominate different systems, but we will focus on two types of interactions that are important in many types of systems: the van der Waals interaction and the electrostatic interaction. The contribution to the osmotic pressure from the van der Waals interaction is obtained by differentiating the expression for the van der Waals free energy of a cell with respect to the number of solvent molecules in the cell. After some mathematical manipulation (see Appendix A) the following simple expression for the van der Waals contribution to the osmotic pressure is obtained:

$$\Pi_{\text{van der Waals}} = -\frac{kT}{V_{agg}} \cdot \frac{z_n \cdot A_{eff}}{36kT} \cdot \left( \frac{\phi^3}{(\phi_{cp} - \phi_{cp}^{1/3}\phi^{2/3})^2} \right), \qquad [26]$$

where $z_n$ is the number of neighboring particles in the cell lattice and $A_{eff}$ symbolizes the effective Hamaker constant in the system. In the examples presented in this paper, we have assumed that the particles are placed in a hexagonal lattice, which means that $z_n$ is twelve in this case.

If the colloidal particles are charged, the electrostatic contribution to the osmotic pressure often dominates and must, of course, be included in the calculations. In the cell model, this contribution to the osmotic pressure can be written as a function of the total ion concentration at the cell boundary:

$$\Pi_{el} = N_A \cdot kT \sum_{i=\text{all ions}} C_i(R), \qquad [27]$$

where $C_i(R)$ is the concentration of ion $i$ at the cell boundary. The boundary concentration $C_i(R)$ can be calculated from the Boltzmann distribution law,

$$C_i(R) = C_i(\text{bulk}) \cdot \exp(-ez_i\Psi(R)/kT), \qquad [28]$$

where $C_i(\text{bulk})$ is the concentration of ion $i$ in a salt solution in equilibrium with the colloidal system, $ez_i$ is the charge of ion $i$ and $\Psi(R)$ is the electrostatic potential at the cell boundary compared with a bulk salt solution without colloidal particles. The cell boundary potential $\Psi(R)$ can be calculated using the Poisson–Boltzmann equation, as in, for example, (48).

Hence, the three contributions to the osmotic pressure in a colloidal dispersion that are used in the subsequent calculations are

$$\Delta\Pi = \Pi_{\text{van der Waals}} + \Pi_{el} + \Pi_{hs}. \qquad [29]$$

In this way, an expression is obtained which gives a good qualitative description of the osmotic pressure in many types of colloidal systems. However, we must point out that $\Delta\Pi$ in Eq. [29] only represents the osmotic pressure due to the colloidal particles and does not include the total osmotic pressure of the solution. The osmotic pressure of, for example, a salt in the solution, is not included in Eq. [29] since low-molecular solutes, e.g., salts, are assumed to freely permeate an ultrafiltration or microfiltration membrane. The resulting osmotic pressure of the low-molecular solute is, therefore, in this case, constant in the boundary layer and across the membrane. In the examples presented in this paper, it is further assumed that the silica particles are totally retained, which is an appropriate assumption when treating silica sols using relatively dense ultrafiltration membranes. In systems where particles are not totally retained, and low-molecular solutes not totally permeable, this can be accounted for by including the permselectivity of the membrane in the calculations.

The magnitude of the different contributions to the osmotic pressure depends on parameters such as the molecular weight (i.e., the size) of the solute, the force of attraction (represented by the Hamaker constant) and the surface potential of the solute/particle. For a dispersion with charged particles, the electrostatic interaction is often the dominating contribution to the osmotic pressure, as shown in Fig. 3.

The osmotic pressure of the particles in a solution is the same, irrespective of the electrolyte concentration in the dispersion, when the osmotic pressure is calculated by the van't Hoff equation. In reality, the electrostatic interaction between the charged particles decreases as the electrolyte con-

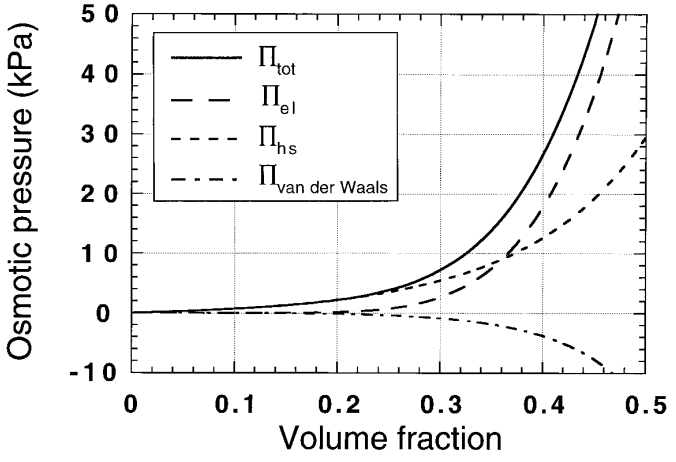


**FIG. 3.** The influence of particle concentration on the osmotic pressure in a silica sol. $\Pi_{el}$, $\Pi_{hs}$, and $\Pi_{van\ der\ Waals}$ denote the osmotic pressure due to repulsive electrostatic forces, the particle entropy, and attractive van der Waals forces, respectively. The surface charge of the particles is −40 mV and the radius is 6 nm. The concentration of NaCl in the silica sol is in equilibrium with a 0.1 *M* bulk solution of NaCl.

centration increases, resulting in a decreased osmotic pressure, as illustrated in Fig. 4.

As shown in Fig. 4, the osmotic pressure due to the silica particles decreases as the salt concentration increases. However, the total osmotic pressure of the dispersion (including the osmotic pressure of the salt) increases, of course, when the salt concentration increases, but, as pointed out earlier, the salt ions are assumed to pass freely through ultrafiltration and microfiltration membranes. Since the transmembrane osmotic pressure gradient due to the salt is zero, it is only the osmotic pressure gradient of the particles that affects the flux.

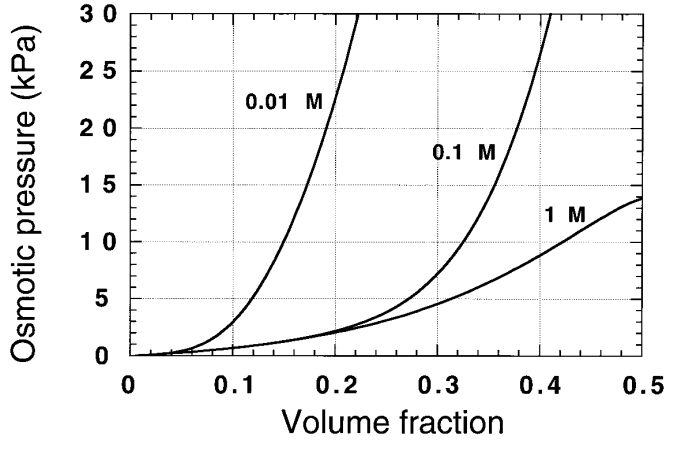


**FIG. 4.** The osmotic pressure due to the silica particles in a dispersion containing 0.01 *M* NaCl (surface potential = −70 mV), 0.1 *M* NaCl (−40 mV), and 1 *M* NaCl (−20 mV), where $T$ = 298 K, $r$ = 6 nm, and $A_{eff} = 1 \times 10^{-20}$ J.

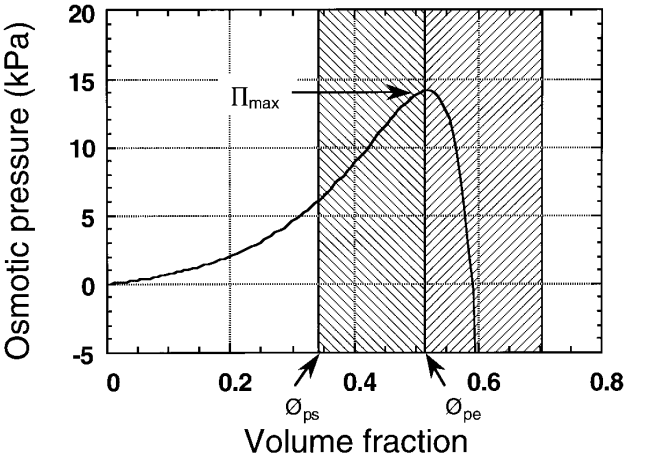


**FIG. 5.** The osmotic pressure versus volume fraction of a silica sol at high salt concentration. The silica particles precipitate instantly beyond a concentration corresponding to the volume fraction $\phi_{pe}$.

### *The Osmotic Pressure in an Unstable Colloidal Dispersion*

The thermodynamic stability of the dispersion was not considered when the influence of different parameters on the osmotic pressure, such as particle concentration, electrolyte concentration, and surface potential, were discussed above. However, a dispersion is often thermodynamically unstable at high salt concentrations, or high dispersion concentrations, and precipitates after a while. There are two critical dispersion concentrations, here denoted $\phi_{ps}$ and $\phi_{pe}$, which must be considered when discussing the precipitation properties of a colloidal system. The dispersion is thermodynamically stable against precipitation at dispersion concentrations below $\phi_{ps}$, even though flocculation may occur in this concentration region. At dispersion concentrations above $\phi_{pe}$ the particles precipitate momentarily, as there is no thermodynamic force to counteract the coagulation of the particles. The dispersion is thermodynamically unstable in the concentration region between $\phi_{ps}$ and $\phi_{pe}$. The precipitation time in this concentration region depends on the energy barrier at $\phi_{pe}$. During ultrafiltration, hysteresis effects occur if the dispersion concentration reaches $\phi_{ps}$ (29). The behavior of an unstable colloidal dispersion is shown in Fig. 5.

## NUMERICAL SOLUTION

To be able to calculate the concentration profile of colloidal particles at the membrane surface, the following parameters must be known:

1. the viscosity of the permeate;
2. the pure water permeability of the membrane, PWP = $J_0/\Delta P_0$;
3. the volume fraction dependence of the frictional coefficient, $f$, used in Eq. [15]; and

4. the volume fraction dependence of the osmotic pressure, $\Delta\Pi$, used in Eq. [21].

In the examples presented in this paper, the frictional coefficients, $f$, were calculated using Eq. [13]. When calculating the osmotic pressure coefficients, $A_i$, the electrostatic contribution to the osmotic pressure was obtained using a computer program that solves the Poisson–Boltzmann equation for different geometries (49).

For given values of the flux, $J$, the operating transmembrane pressure, $\Delta P$, and concentration of particles in the bulk solution, $\phi_b$, the concentration profile is calculated in the following manner.

1. The osmotic transmembrane pressure difference is calculated from Eq. [2].

$$\Delta\Pi = \Delta P - J/\mathrm{PWP} = \Delta P - J\cdot\Delta P_0/J_0. \quad [30]$$

2. If the osmotic transmembrane pressure difference, calculated from the relation above, exceeds the osmotic pressure beyond which the colloidal particles precipitate, $\Delta\Pi_{max}$, a filter cake of precipitated particles will be built up at the membrane surface. The above relation must then be modified as follows:

2.1 The total osmotic pressure difference, across both the membrane and the filter cake, is $\Delta\Pi_{max}$, and

2.2 The thickness of the filter cake is calculated from Eq. [14]

$$\Delta L_{cake} = \frac{\Delta P_{cake}\cdot V_{agg}}{f(\phi_{cake})\cdot\phi_{cake}\cdot J}, \quad \text{where}$$

$$\Delta P_{cake} = \Delta P - \Delta\Pi_{max} - J/\mathrm{PWP} \quad [31]$$

and $\phi_{cake}$ is the volume fraction of particles in the cake.

3. The volume fraction of colloidal particles at the membrane surface (or the cake, if there is one) is calculated from the osmotic pressure difference across the membrane (and the cake) using Eq. [20]. This calculation is most easily performed using the Newton–Raphson method (50).

4. The concentration interval, $\phi_{membrane} \rightarrow \phi_{bulk}$ is divided into an appropriate number of equal intervals (100 in this paper) and the length of each interval is calculated from Eq. [22] to be

$$\Delta x_j = \int_{\phi_{aj}+(\Delta\phi/2)}^{\phi_{aj}-(\Delta\phi/2)} \frac{dx}{d\phi}\,d\phi \approx \frac{kT}{6\pi\eta_0 r J}\cdot\frac{(1-\phi_{aj})^3\cdot(1+\Sigma_{i=2}\,A_i i\phi_{aj}^{i-1})}{\Sigma_{i=0}\,f_i\phi_{aj}^i} \times \ln\left(\frac{\phi_{aj}-\phi_p+(\Delta\phi/2)}{\phi_{aj}-\phi_p-(\Delta\phi/2)}\right), \quad [32]$$

where $\phi_{aj}$ is the volume fraction in the middle of the concentration interval $j$.

5. The concentration profile and the thickness of the boundary layer can now be determined based on the division of the boundary layer performed in point 4 above.

6. In the calculations, points 1–5 above, the flux was assumed to be known. If instead, the flux is to be calculated the thickness of the boundary layer must be known. The thickness of the boundary layer may, as an approximation, be assumed to only be influenced by the shear rate, and not the concentration or the applied transmembrane pressure. This means that only one experiment is needed to obtain the boundary layer thickness at a specific experimental shear rate. The calculated thickness can then be used in the theoretical model when studying the influence of different operating parameters, provided that the shear rate and the module are the same as in the experiment, of course.

The flux is calculated by the following procedure: A flux value is assigned and the calculations in points 1–5 are performed. If the calculated thickness of the boundary layer agrees with the given thickness, then the calculated flux value is correct. If the values of the thickness do not agree, a new flux is assumed and the calculations are repeated. If a regula falsi procedure is used when choosing a new flux value, the correct flux is soon found (50).

An easy-to-use computer program based on the above principles can be downloaded from the web site address http://www.membfound.lth.se/chemeng1.html at Internet.

## RESULTS

The model presented in this paper has two main advantages. First, this model combines the ability of the osmotic pressure model to predict the performance of solutions containing low-molecular, noninteracting solutes and the cake filtration model which is commonly used when solutions with larger, interacting solutes are considered. Second, the concentration profile calculated by the new force balance model gives a more realistic view of the concentration in the boundary layer at the membrane than the other two models. The concentration gradient at the membrane, calculated by the three models, is shown in Fig. 6.

The influence of some operating parameters on the flux and the concentration profile will now be demonstrated.

### *Influence of Operating Pressure*

The flux in a membrane process increases almost linearly with increasing transmembrane pressure at low operating pressures. The flux increase then levels off as the operating pressure increases, as shown in the inset in Fig. 7. The leveling off of the flux is due to an increased hydraulic resistance in the boundary layer at high pressures (see Fig. 7).

For the operating conditions used in the example shown

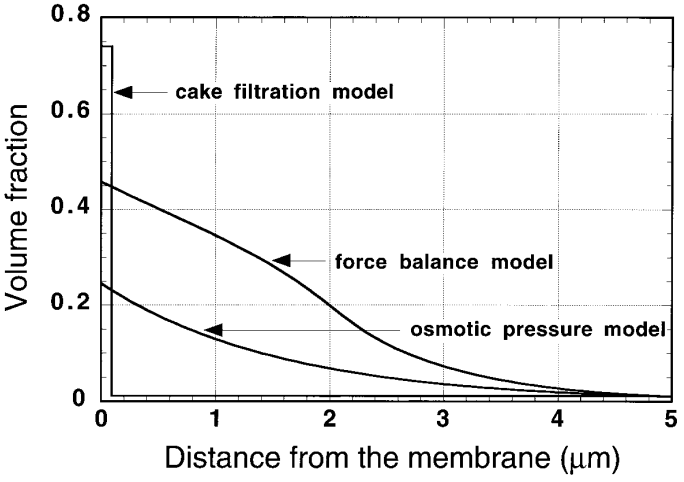


**FIG. 6.** Concentration profile of a 0.1 *M* NaCl silica sol calculated with the new force balance model, the osmotic pressure model, and the cake filtration model. The calculations were based on the following operating parameters: PWP = 2000 l m$^{-2}$ h$^{-1}$ MPa$^{-1}$ at 25°C, $\Delta P$ = 100 kPa, $T$ = 25°C, $\phi_b$ = 0.01 (i.e., $C_b$ = 2.5 wt%), and $r$ = 6 nm.

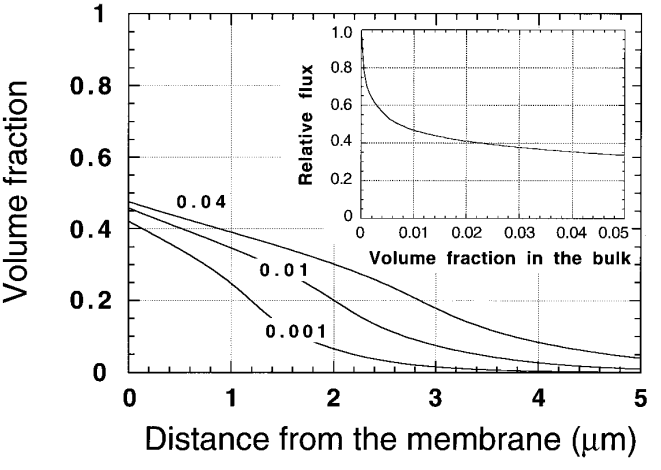


**FIG. 8.** The influence of the bulk particle concentration on the concentration profile for a 0.1 *M* NaCl silica sol. The bulk solution volume fractions 0.001, 0.01, and 0.04 correspond to 0.25, 2.5 and 10 wt%, respectively. The calculations are based on the following operating parameters: PWP = 2000 l m$^{-2}$ h$^{-1}$ MPa$^{-1}$ at 25°C, $\Delta P$ = 100 kPa, $T$ = 25°C, $r$ = 6 nm, and a fluid shear in the module corresponding to a boundary layer thickness of 5 $\mu$m.

in Fig. 7, the critical precipitation concentration, $\phi_{pe}$ (often referred to as the gel concentration), is reached at the membrane surface when the operating pressure is 700 kPa. At pressures above 700 kPa the thickness of the gel layer increases, but the concentration profile outside this layer is unchanged.

*Influence of Concentration*

The flux is reduced as the concentration in the bulk solution increases. This flux reduction is caused by an increased hydraulic resistance in the boundary layer, just as when the pressure is increased. However, there is an important difference between how an increase in the pressure and an increase in the bulk concentration affects the concentration profile. Increasing the pressure results in a substantial increase in the volume fraction (i.e., densification) of the material at the membrane surface, whereas when the bulk concentration increases only a minor increase in the volume fraction in the immediate vicinity of the membrane is observed, as shown in Fig. 8.

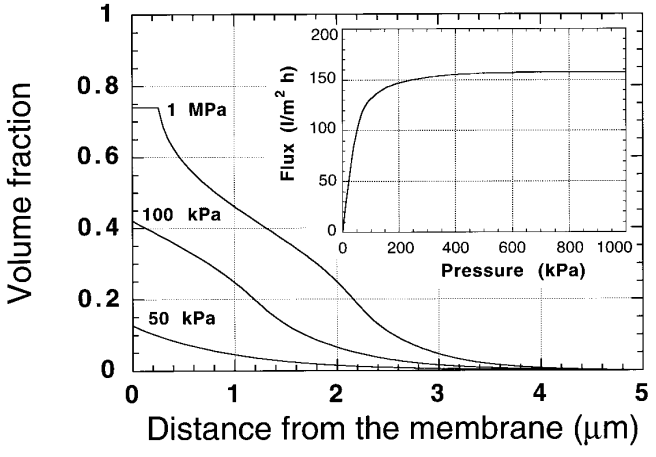


**FIG. 7.** The influence of the operating transmembrane pressure on the concentration profile for a 0.1 *M* NaCl silica sol. The bulk solution volume fraction is 0.001 which corresponds to 0.25 wt%. The calculations are based on the following operating parameters: PWP = 2000 l m$^{-2}$ h$^{-1}$ MPa$^{-1}$ at 25°C, $T$ = 25°C, $r$ = 6 nm, and a fluid shear in the module corresponding to a boundary layer thickness of 5 $\mu$m.

*Influence of Particle Size*

The flux is reduced as the particle size increases. However, this flux reduction is observed only for particles of a limited size. When the particles become larger, additional effects, such as shear-induced diffusion and inertial lift, start to become important. For silica particles, Fane (51) found a flux minimum at 0.1 $\mu$m and Lahoussine-Turcaud *et al.* (52) found a minimum at 0.2 $\mu$m. The maximum particle radius in Fig. 9 is definitely below these threshold particle sizes where the shear-induced diffusivity starts to become important.

The concentration at the membrane surface increases as the particle size increases, and when treating large particles a cake is built up at the membrane surface. Although the concentration at the membrane surface is much higher when treating a solution with 20-nm silica particles than 10-nm particles, the flux is not so drastically reduced as could be expected. This is due to the fact that the flow channels in the boundary layer of accumulated material at the membrane surface are larger when the particle size increases and the

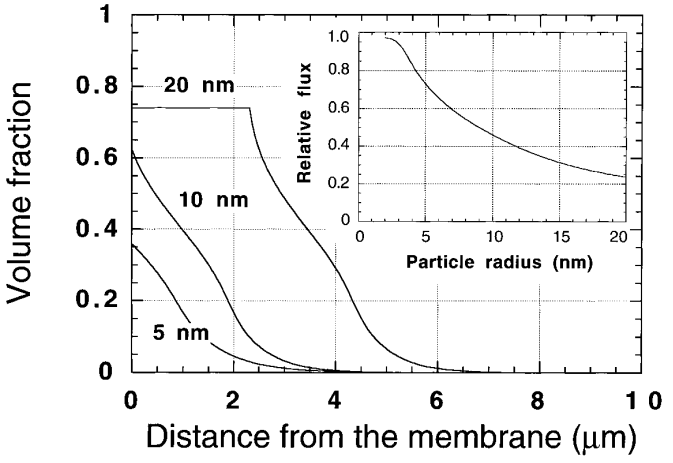


**FIG. 9.** The influence of varying particle size on the concentration profile during ultrafiltration of a 0.1 *M* NaCl silica sol. The bulk solution volume fraction is 0.001 which corresponds to 0.25 wt%. The calculations are based on the following operating parameters: PWP = 2000 l $m^{-2}$ $h^{-1}$ $MPa^{-1}$ at 25°C, $\Delta P$ = 100 kPa, $T$ = 25°C, and a fluid shear in the module corresponding to a boundary layer thickness of 5 $\mu$m.

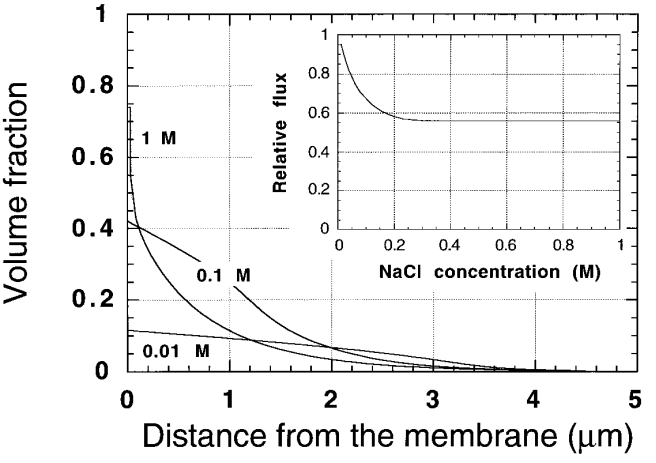


**FIG. 10.** Influence of varying electrolyte concentration on the concentration profile during ultrafiltration of a silica sol. The bulk solution volume fraction is 0.001 which corresponds to 0.25 wt%. The calculations are based on the following operating parameters: PWP = 2000 l $m^{-2}$ $h^{-1}$ $MPa^{-1}$ at 25°C, $\Delta P$ = 100 kPa, $T$ = 25°C, $r$ = 6 nm, and a fluid shear in the module corresponding to a boundary layer thickness of 5 $\mu$m.

specific hydraulic resistance of the boundary layer is consequently reduced.

In this example, the silica sol was assumed to be monodisperse. When treating a mixture of particles of different sizes, calculation of the concentration profile becomes more complicated. The overall packing density in the concentrated layer increases as a consequence of the variation in particle size, and therefore the resistance to permeation is enhanced. The extent of this effect depends on the particle diameter ratio and the type of packing. The effect of nonuniformity of cell size and random orientation of nonsymmetrical objects has been treated by Jönsson (53). Another particle size problem arises when the surface potential of the particles is low, and particles flocculate, as the aggregate size then becomes indeterminate (54).

### *Influence of Electrolyte Concentration*

The electrostatic repulsion between molecules/particles in a solution depends both on the nature of the molecules/particles and on operational parameters such as pH and ionic strength of the solution. Flux is reduced as the electrostatic repulsion diminishes, as shown in Fig. 10, where the electrostatic repulsion is varied by altering the ionic strength (i.e., the electrolyte concentration) in a silica sol. The flux decrease experienced when the electrostatic repulsion decreases is due to the increase in the flow resistance when the material in the boundary layer becomes more closely packed as a result of decreased repulsion between the particles.

At a low electrolyte concentration where the electrostatic repulsion is large, the concentration gradient is almost linear (see Fig. 10) and the concentration at the surface of the membrane is relatively low. The concentration at the membrane surface increases as the electrostatic repulsion decreases. At higher electrolyte concentrations, a cake is formed at the membrane surface, and the flux then reaches a plateau value.

### *Influence of Fluid Shear*

The operational parameter that has the largest impact on the boundary layer thickness is the fluid shear in the membrane module. The most common way of enhancing the fluid shear is by increasing the cross-flow velocity. However, high

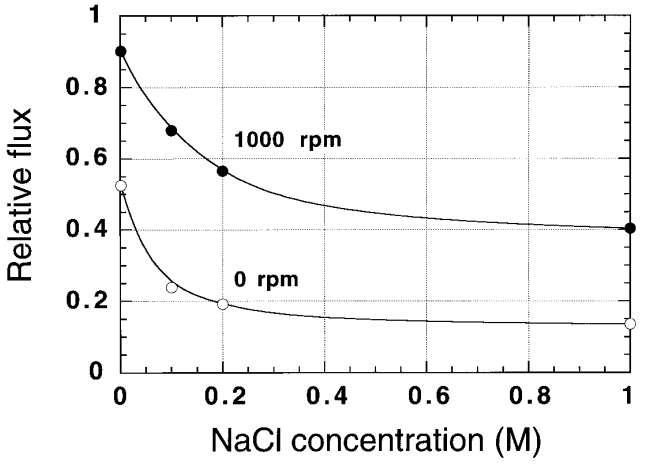


**FIG. 11.** The influence of rotary speed on flux during ultrafiltration of a silica sol. Experimental results from (29). The bulk solution volume fraction was 0.0016 which corresponds to 0.4 wt%. The relative flux is the flux divided by the pure water flux after cleaning and conditioning of the membrane (PES25 from Hoechst) for 12 h. The pure water flux was 2600 l $m^{-2}$ $h^{-1}$ $MPa^{-1}$ at 25°C, the radius of the spherical silica particles (Ludox HS-40 from DuPont) was 6 nm, and the operating pressure was 100 kPa.

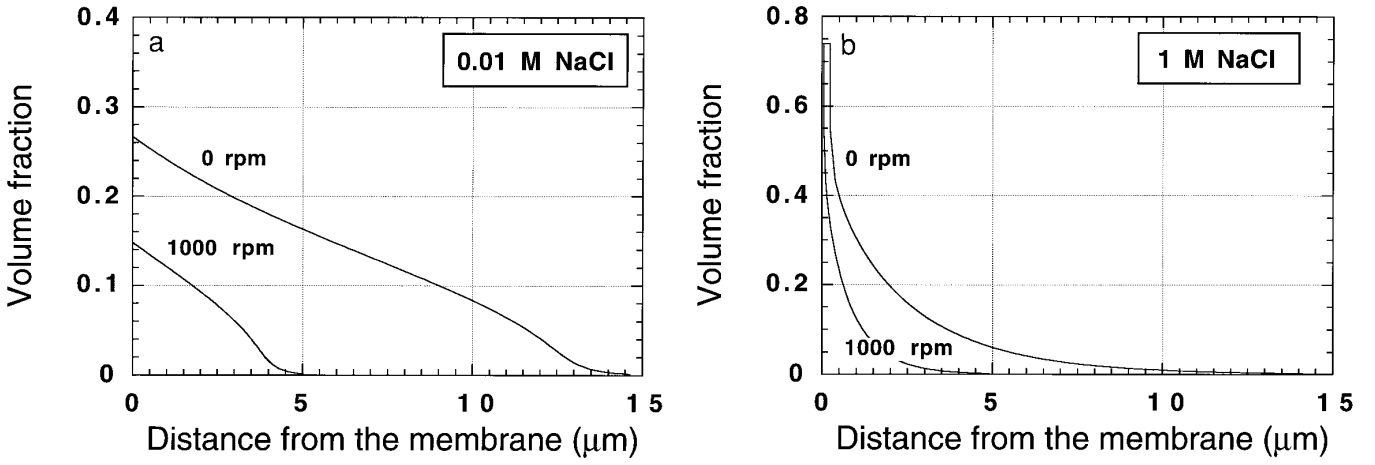


**FIG. 12.** Concentration profile at low and high electrolyte concentration during ultrafiltration of a silica sol. The calculations are based on the experimentally measured flux values given in the legend to Fig. 11.

cross-flow velocities generate high pressure drops. When studying the influence of fluid shear on flux, rotary modules are therefore often used (55–61), as the shear generation and operating pressures are independent of each other in this type of module. The flux of a silica sol at two rotary speeds is shown in Fig. 11.

The concentration profiles at the two rotary speeds resemble the profiles in Fig. 10. However, the boundary layer thickness and the concentration in the boundary layer increase as the rotary speed decreases. The calculated concentration profiles at the extremes, 0.01 and 1 *M* NaCl, and 0 and 1000 rpm, respectively, can be seen in Fig. 12 (observe the difference in scale on the *y*-axis of the two curves).

Both the concentration at the membrane surface and the boundary layer thickness increase when the rotary speed is reduced. In the 0.01 *M* silica sol there is a marked concentration increase in the whole boundary layer, whereas in the 1 *M* NaCl silica sol it is primarily the increased thickness of the cake at the membrane that reduces the flux when the rotary speed is decreased.

## SUMMARY

As a rule, the treatment of solutes causes an instantaneous reduction in flux relative to the pure water flux of the membrane. Three major phenomena cause this flux reduction. (i) A concentrated layer of solute compounds retained at the surface of the membrane is formed as soon as the transport of solvent through the membrane commences and a hydraulic resistance in series with the membrane is thus established. (ii) Pores are physically blocked by solute compounds/particles. (iii) Solute molecules are adsorbed onto the pore walls in the interior of the membrane, leading to pore narrowing. The first phenomenon, concentration polarization, is usually the dominating flux inhibitor.

Concentration polarization is usually ascribed either to a reduction in the effective thermodynamic driving force due to the increased osmotic pressure difference across the membrane or to an increase in total hydraulic resistance due to the formation of a less permeable phase, a cake/gel, in series with the membrane. These two conditions are usually described by the osmotic pressure model and the cake filtration model. However, these models only apply under limited operating conditions. The force balance model presented in this paper combines the basic concepts of the osmotic pressure model and the cake filtration model into one single fluid flow model. This new model is based on basic relations describing interactions between colloidal aggregates and the theory of fluid flow in concentrated dispersions. The force balance model allows the flux to be calculated under different operating conditions, treating both macromolecules and colloidal particles. The concentration profile at the membrane surface is also easily derived.

The force balance model includes particle–particle interactions, such as attractive van der Waals forces and repulsive electrostatic forces, which allows the study of the influence of different solutions properties, such as pH and ionic strength, on the flux and concentration profiles. The operating conditions under which the critical precipitation concentration (the gel, or cake, concentration) is reached can also be calculated.

## APPENDIX A

The van der Waals interaction between two spherical particles can be expressed as (62)

$$W_{\text{agg-agg}} = -\frac{A_{\text{eff}}}{6}\left(\frac{0.5}{u-1}+\frac{0.5}{u}+\ln\left(1-\frac{1}{u}\right)\right),$$

$$\text{where}\quad u=\left(\frac{r+L}{r}\right)^2. \quad [A1]$$

$A_{\text{eff}}$ denotes the effective Hamaker constant, $r$ is the radius of the spherical particles, and $2L$ is the distance between two spherical particles.

For a concentrated dispersion of spherical particles, in which every particle is surrounded by many other particles, the total van der Waals energy in the system may be estimated as the sum of the van der Waals interactions between neighboring particles. Equation [A1] can be used to describe the interaction between a particle and its neighboring particles. The error that is introduced when the interactions are limited to only the neighboring particles, and all particles in the system are not included, is usually relatively small as the van der Waals interactions decrease relatively quickly as a function of the distance between the particles, especially when the distance exceeds one particle diameter. Introducing these approximations, the van der Waals interaction per particle can be written as

$$W_{\text{van der Waals}} \approx \frac{z_n N_{\text{agg}}}{2} W_{\text{agg-agg}}, \qquad [A2]$$

where $z_n$ is the number of neighboring particles around one cell.

To be able to use Eq. [A1] to calculate $W_{\text{agg-agg}}$, the parameter $u$ must be specified for the system under consideration. If the particles in the system are placed in a lattice where the distance between the lattice points depends on the concentration of the colloidal particles, but the geometry of the lattice is not affected by the concentration, the parameter $u$ can be written as

$$u = \left(\frac{\phi_{\text{cp}}}{\phi}\right)^{2/3} \qquad [A3]$$

The contribution to the osmotic pressure from the van der Waals interactions is obtained by differentiating the expression for $W_{\text{van der Waals}}$ with respect to the number of solvent molecules in the system.

$$\begin{aligned}\Pi_{\text{van der Waals}} &= -\frac{1}{V_w}\left(\frac{\partial W_{\text{van der Waals}}}{\partial N_w}\right)_{N_{\text{agg}}} \\ &= -\frac{z_n N_{\text{agg}}}{2V_w}\left(\frac{\partial W_{\text{agg-agg}}}{\partial N_w}\right)_{N_{\text{agg}}} \\ &= -\frac{z_n N_{\text{agg}}}{2V_w}\left(\frac{dW_{\text{agg-agg}}}{du}\right)\left(\frac{\partial u}{\partial N_w}\right)_{N_{\text{agg}}} \\ &= -\frac{z_n A_{\text{eff}} N_{\text{agg}}}{24V_w(u(u-1))^2}\left(\frac{\partial u}{\partial N_w}\right)_{N_{\text{agg}}}. \qquad [A4]\end{aligned}$$

When the expression for $(\partial u/\partial N_w)$

$$\left(\frac{\partial u}{\partial N_w}\right)_{N_{\text{agg}}} = \phi_{\text{cp}}^{2/3}\left(\frac{\partial}{\partial N_w}\left(\frac{N_{\text{agg}}V_{\text{agg}} + N_w V_w}{N_{\text{agg}}V_{\text{agg}}}\right)^{2/3}\right)_{N_{\text{agg}}} = \frac{2\phi_{\text{cp}}^{2/3}V_w\phi^{1/3}}{3N_{\text{agg}}V_{\text{agg}}} \qquad [A5]$$

is introduced in Eq. [A4] the following simple relation for $\Pi_{\text{van der Waals}}$ is obtained:

$$\Pi_{\text{van der Waals}} = -\frac{kT}{V_{\text{agg}}}\cdot\frac{z_n\cdot A_{\text{eff}}}{36kT}\cdot\left(\frac{\phi^3}{(\phi_{\text{cp}} - \phi_{\text{cp}}^{1/3}\phi^{2/3})^2}\right). \qquad [A6]$$

## APPENDIX B: NOTATION

| | |
|---|---|
| $A_{\text{eff}}$ | effective Hamaker constant ($J$) |
| $A_i$ | osmotic pressure coefficient |
| $bM$ | difference in mass between particle and displaced solvent (kg) |
| $C$ | solute concentration (mol $m^{-3}$) |
| $C_b$ | solute concentration in the bulk (mol $m^{-3}$) |
| $C_i(R)$ | concentration of ion $i$ at the cell boundary (mol $m^{-3}$) |
| $C_m$ | solute concentration at the membrane surface (mol $m^{-3}$) |
| $C_p$ | solute concentration in the permeate (mol $m^{-3}$) |
| $D$ | diffusion coefficient ($m^2$ $s^{-1}$) |
| $D_0$ | diffusion coefficient in a dilute dispersion ($m^2$ $s^{-1}$) |
| $e$ | unit charge (As) |
| $F_{ff}$ | drag force (N) |
| $F_{tf}$ | thermodynamic force (N) |
| $f$ | frictional coefficient (Pa s m) |
| $f_0$ | frictional coefficient in a dilute dispersion (Pa s m) |
| $f_i$ | frictional coefficient (Pa s m) |
| $h_D$ | mass transfer coefficient (m $s^{-1}$) |
| $J$ | flux (l $m^{-2}$ $h^{-1}$) |
| $J_0$ | pure water flux (l $m^{-2}$ $h^{-1}$) |
| $k$ | Boltzmann constant (J $K^{-1}$) |
| $2L$ | distance between two particles (m) |
| $\Delta L$ | layer thickness (m) |
| $N_A$ | Avogadro's number ($mol^{-1}$) |
| $N_{\text{agg}}$ | number of particles |
| $N_w$ | number of water molecules |
| $\Delta P$ | transmembrane pressure difference (Pa) |
| $\Delta P_{\text{cake}}$ | pressure difference across the cake (Pa) |
| $\Delta P_0$ | transmembrane pressure difference when the pure water flux is measured (Pa) |
| PWP | pure water permeability (l $m^{-2}$ $h^{-1}$ $MPa^{-1}$) |
| $R_c$ | hydraulic resistance of the cake ($m^{-1}$) |
| $R_m$ | hydraulic resistance of the membrane ($m^{-1}$) |

| | |
|---|---|
| $r$ | radius of a particle (m) |
| $S$ | sedimentation constant (mol s) |
| $T$ | absolute temperature (K) |
| $V_{agg}$ | volume of a particle ($m^3$) |
| $V_w$ | volume of a solvent molecule ($m^3$ $mol^{-1}$) |
| $v$ | fluid velocity relative to the particles (m $s^{-1}$) |
| $x$ | distance from the membrane surface (m) |
| $z_i$ | counterion charge number |
| $z_n$ | number of neighboring particles at close packing |

*Greek*

| | |
|---|---|
| $\delta$ | thickness of the boundary layer (m) |
| $\eta$ | viscosity (Pa s) |
| $\eta_0$ | viscosity of the solvent (Pa s) |
| $\mu$ | chemical potential (J $mol^{-1}$) |
| $\mu_{agg}$ | chemical potential of particles in the solution (J $mol^{-1}$) |
| $\mu_w$ | chemical potential of water (J $mol^{-1}$) |
| $\Pi$ | total osmotic pressure (Pa) |
| $\Pi_{el}$ | osmotic pressure due to electrostatic contributions (Pa) |
| $\Pi_{hs}$ | osmotic pressure due to the entropy of mixing (Pa) |
| $\Pi_{max}$ | osmotic pressure at which particle precipitation starts (Pa) |
| $\Pi_{van\ der\ Waals}$ | osmotic pressure due to attractive interaction forces between particles (Pa) |
| $\Delta\Pi$ | transmembrane osmotic pressure difference (Pa) |
| $\Psi(R)$ | electrostatic potential at the cell boundary (V) |
| $\phi$ | volume fraction of particles |
| $\phi_{cake}$ | volume fraction of particles in the cake |
| $\phi_{cp}$ | volume fraction that particles occupy at close packing |
| $\phi_{hs}$ | volume fraction of hard spheres |
| $\phi_p$ | volume fraction of particles in the permeate |
| $\phi_{pe}$ | critical volume fraction at which particles instantly precipitate |
| $\phi_{ps}$ | critical volume fraction at which precipitation starts |

## ACKNOWLEDGMENT

A.-S.J. was partly financed by a grant from the Swedish Research Council for Engineering Sciences.

## REFERENCES


1. Pepper, D., *Desalination* **77,** 55 (1990).
2. Rautenbach, R., and Gröschl, A., *Desalination* **77,** 73 (1990).
3. Jönsson, A.-S., and Trägårdh, G., *Desalination* **77,** 135 (1990).
4. Horst, H. C. v. d., and Hanemaaijer, J. H., *Desalination* **77,** 235 (1990).
5. Zydney, A. L., *J. Membr. Sci.* **68,** 183 (1992).
6. Mackley, M. R., and Sherman, N. E., *J. Membr. Sci.* **77,** 113 (1993).
7. Petsev, D. N., Starov, V. M., and Ivanov, I. B., *Colloids Surf. A Physicochem. Eng. Aspects* **81,** 65 (1993).
8. Belfort, G., Davis, R. H., and Zydney, A. L., *J. Membr. Sci.* **96,** 1 (1994).
9. Bouchard, C. R., Carreau, P. J., Matsuura, T., and Sourirajan, S., *J. Membr. Sci.* **97,** 215 (1994).
10. Chang, D.-J., Hsu, F.-C., and Hwang, S.-J., *J. Membr. Sci.* **98,** 97 (1995).
11. Welsch, K., McDonogh, R. M., Fane, A. G., and Fell, C. J. D., *J. Membr. Sci.* **99,** 229 (1995).
12. Bowen, W. R., and Jenner, F., *Chem. Eng. Sci.* **50,** 1707 (1995).
13. Jönsson, B., and Wennerström, H., *J. Colloid Interface Sci.* **80,** 482 (1981).
14. Jönsson, B., and Wennerström, H., *J. Phys. Chem.* **91,** 338 (1987).
15. Happel, J., *AIChE J.* **4,** 197 (1958).
16. Jönsson, B., Wennerström, H., Nilsson, P.-G., and Linse, P., *Colloid Polym. Sci.* **264,** 77 (1986).
17. Blatt, W. F., Dravid, A., Michaels, A. S., and Nelsen, L., *in* ''Membrane Science and Technology'' (J. E. Flinn, Ed.), p. 47. Plenum, New York, 1970.
18. Kozinski, A. A., and Lightfoot, E. N., *AIChE J.* **18,** 1030 (1972).
19. Vilker, V. L., Colton, C. K., and Smith, K. A., *AIChE J.* **27,** 637 (1981).
20. Jonsson, G., *Desalination* **51,** 61 (1984).
21. Wijmans, J. G., Nakao, S., and Smolders, C. A., *J. Membr. Sci.* **20,** 115 (1984).
22. Wijmans, J. G., Nakao, S., Berg, J. W. A. v. d., Troelstra, F. R., and Smolders, C. A., *J. Membr. Sci.* **22,** 117 (1985).
23. Berg, G. B. v. d., and Smolders, C. A., *Desalination* **77,** 101 (1990).
24. Nabetani, H., Nakajima, M., Watanabe, A., Nakao, S., and Kimura, S., *AIChE J.* **36,** 907 (1990).
25. Vilker, V. L., Colton, C. K., and Smith, K. A., *J. Colloid Interface Sci.* **79,** 548 (1981).
26. Bird, R. B., Stewart, W. E., and Lightfoot, E. N., ''Transport Phenomena.'' Wiley, New York, 1960.
27. Dejmek, P., ''Concentration Polarization in Ultrafiltration of Micromodules.'' Ph.D. thesis, Lund Institute of Technology, Lund, Sweden, 1975.
28. Davis, K. E., and Russel, W. B., *Phys. Fluids A* **1,** 82 (1989).
29. Jönsson, A.-S., and Jönsson, B., accepted for publication in Sep. *Sci. Techn.*
30. Green, G., and Belfort, G., *Desalination* **35,** 129 (1980).
31. Davis, R. H., and Leighton, D. T., *Chem. Eng. Sci.* **42,** 275 (1987).
32. Romero, C. A., and Davis, R. H., *J. Membr. Sci.* **62,** 249 (1991).
33. Schmitz, P., Wandelt, B., Houi, D., and Hildenbrand, M., *J. Membr. Sci.* **84,** 171 (1993).
34. Atkins, P. W., ''Physical Chemistry.'' Oxford Univ. Press, Oxford, 1994.
35. Parkhurst, H. J., and Jonas, J., *J. Chem. Phys.* **63,** 2698 (1975).
36. Hynes, J. T., *Annu. Rev. Phys. Chem.* **28,** 301 (1977).
37. Hiemenz, P. C., ''Principles of Colloid and Surface Chemistry.'' Dekker, New York, 1986.
38. Hunter, R. J., ''Zeta Potential in Colloid Science.'' Academic Press, London, 1981.
39. Altena, F. W., ''Phase Separation Phenomena in Cellulose Acetate Solutions in Relation to Assymetric Membrane Formation.'' Ph.D. thesis, Twente University of Technology, Enschede, The Netherlands, 1982.
40. Vesluijs, C. W., and Smit, J. A. M., *J. Membr. Sci.* **14,** 229 (1983).
41. Vilker, V. L., Colton, C. K., Smith, K. A., and Green, D. L., *J. Membr. Sci.* **20,** 63 (1984).
42. Israelachvili, J., ''Intermolecular and Surface Forces.'' Academic Press, London, 1991.
43. McQuarrie, D. A., ''Statistical Mechanics.'' Harper & Row, New York, 1976.
44. Hill, T. L., ''Statistical Mechanics.'' Addison & Wesley, Reading, MA, 1960.

45. Landgren, M., ''Thermodynamic Modelling of Ionic Surfactant Systems.'' Ph.D. thesis, Lund University, Lund, Sweden, 1990.
46. Carnahan, N. F., and Starling, K. E., *J. Chem. Phys.* **53,** 600 (1970).
47. Jönsson, K. A.-S., and Jönsson, B. T. L., *AIChE J.* **38,** 1340 (1992).
48. Gunnarsson, G., Jönsson, B., and Wennerström, H., *J. Phys. Chem.* **84,** 3114 (1980).
49. Web-site address: http://www.membfound.lth.se/chemeng1.html.
50. Arfken, G., ''Mathematical Methodes for Physicists.'' Academic Press, New York, 1968.
51. Fane, A. G., *J. Membr. Sci.* **20,** 249 (1984).
52. Lahoussine-Turcaud, V., Wiesner, M. R., and Bottero, J.-Y., *J. Membr. Sci.* **52,** 173 (1990).
53. Jönsson, A.-S., ''A New Method for the Estimation of Residual Lignin Content in Paper Pulp.'' Ph.D. thesis, Lund Institute of Technology, Lund, Sweden, 1983.
54. McDonogh, R. M., Welsch, K., Fane, A. G., and Fell, C. J. D., *Desalination* **70,** 251 (1988).
55. Lopez-Leiva, M., ''Ultrafiltration in Rotary Annular Flow.'' Ph.D. thesis, Lund Institute of Technology, Lund, Sweden, 1979.
56. Riesmeier, B., Kroner, K. H., and Kula, M.-R., *Desalination* **77,** 219 (1990).
57. Holeschovsky, U. B., and Cooney, C. L., *AIChE J.* **37,** 1219 (1991).
58. Murase, T., Iritani, E., Chidphong, P. K., Kano, K. A., and Shirato, M., *Int. Chem. Eng.* **31,** 370 (1991).
59. Belfort, G., Pimbley, J. M., Greiner, A., and Chung, K. Y., *J. Membr. Sci.* **77,** 1 (1993).
60. Belfort, G., Mikulasek, P., Pimbley, J. M., and Chung, K. Y., *J. Membr. Sci.* **77,** 23 (1993).
61. Jönsson, A.-S., *J. Membr. Sci.* **79,** 93 (1993).
62. Mahanty, J., and Ninham, B. W., ''Dispersion Forces.'' Academic Press, New York, 1976.